The relations between the histopathological findings and x-ray images of augmented bone after the guided bone regeneration

（骨再生誘導法後の骨造成における病理組織学的所見および
エックス線画像との関連性）

日本大学松戸歯学研究科歯学専攻

樋口 真弘

（指導：久山　佳代 教授）

This paper is summary thesis of

Masahiro Higuchi, Masaaki Suemitsu, Tsuyoshi Tanaka et al., Correlation Between Radiological Interpretation and Histopathological Findings of Bone Augmentation Area After Guided Bone Regeneration：A Comparative Study, Journal of Japanese Society for Dental Products. 32(1), 16-25, 2018

and

Masahiro Higuchi, Masaaki Suemitsu, Tsuyoshi Tanaka et al., Examination of the Efficacy of Micro-computed Tomography for the Evaluation of Bone Augmentation Following Guided Bone Regeneration, Journal of Japanese Society for Dental Products.32(2), in press.

Contents

Abstract

The purpose of the present study was to contrast histopathological, radiological and micro-CT findings within the bone augmentation area after guided bone regeneration (GBR) in study 1 and 2. Besides, it was to examine conditions for setting threshold values in digital image evaluation of reconstructed images from micro-CT in study 2. Eight (study 1) and 18 (study 2) patients who had lost teeth and underwent GBR using non-absorbable anorganic bovine bone (ABB) graft material was the study subjects. At the time of implant surgery, bone core biopsy samples were offered to histopathological examination. Digital and histopathological and micro-CT component ratios were calculated using ImageJ 1.51i image analysis software. Bone core samples comprised new bone, osteoid, bone graft materials and connective tissue.

In study 1, because of the bone graft materials remaining amount, mean area ratios for these 4 components were 2.50%, 3.50%, 38.73% and 55.47% with the large pattern, 19.45%, 0.30%, 24.10% and 56.20% with the moderate pattern, and 26.53%, 13.53%, 2.53%, and 57.27% with the small pattern, respectively. The relative concentration ratios of the bone augmentation area compared to the existing area of dental radiographic images were calculated for dental films. In dental radiographic image analysis, the mean relative concentration ratio

was 0.92, and no significant variability was evident among the eight cases. A significant correlation was indicated between the relative concentration ratio and the hard tissue area ($p<0.001$).

In study 2, mean body mineral density (BMD) was 628.11±58.00 mg/mm^3 (range, 535.50-783.10 mg/mm^3). Mean ratio of the hard tissue component from digital images was 20.09±4.91% (range, 14.38-32.59%). Strong correlations were apparent between BMD and both digital micro-CT and histopathological hard tissue area (new bone and bone graft materials) ratios (correlation coefficients, 0.923 and 0.938, respectively; $p<0.01$ each). A positive correlation between digital micro-CT image and histopathological hard tissue ratio (0.875) was also confirmed ($p<0.01$).

New bone and/or reorganization with non-absorbable ABB graft materials were observed in the bone augmentation area after GBR, and radiological interpretations by dentists were influenced by these hard tissue areas but no significant variability. Micro-CT image can be clinically useful to evaluate bone quality within bone augmentation areas after GBR.

Key words：Bone Augmentation，Guided Bone Regeneration（GBR），X-ray Image，Histopathological

findings, Micro-computed Tomography (Micro-CT）, Body Mineral Density (BMD）

Introduction

Guided bone regeneration (GBR) has been developed for cases with insufficient bone volume, to expand the indications for dental implant treatment [1]. Bone mineral density (BMD) is of extreme importance to primary implant stability, particularly when considering either the immediate load or the early loading protocol after GBR [2]. Several techniques are available for evaluating bone density, including histomorphometric analysis [1,3], the tactile sense of the surgeon [1,4], and radiological evaluation [1,5]. Among these, conventional two-dimensional radiography is used for evaluating bone density at the dental chair side, because dental cone-beam computed tomography has not been widely adopted by dental clinics in Japan [6]. Some radiological studies concerning the period of bone augmentation after GBR have also been reported. X-ray evaluations of bone augmentation after GBR have been performed using analysis of new bone height [7-9]. However, studies correlating radiological interpretations and histopathological findings are scarce, and no clear histopathological evidence has been reported for bone augmentation in comparison to radiological image findings after GBR.

To observe the hard tissue core biopsy histopathologically, it may take time and expertise to sample preparation. In contrast, micro-computed tomography (micro-CT) offers the advantage of being able to be

performed immediately after collection of the biopsy core sample without decalcification. Digital image evaluation using micro-CT of the bone augmentation area has been reported for animal models [10-13], and studies comparing micro-CT and histopathological observations for the bone augmentation area have been reported [11,14,15]. However, correlations between the results of component analysis from micro-CT and histomorphology have yet to be reported. The patient can understand the effect of GBR by showing three-dimensional (3D) image reorganization of bone augmentation area. Further, it may be useful for determination of implant superstructure attachment time.

The purpose of the present study was to contrast histopathological, radiological and micro-CT findings within the bone augmentation area after GBR. Besides, it was to examine conditions for setting threshold values in digital image evaluation of reconstructed images from micro-CT.

Materials and Methods

1. Subjects (study 1,2)

All patients received a description of implant treatment after GBR and the purposes of the present study from September 2016 to June 2017 (study 1, 362 patients) and March 2017 to June 2018 (study 2, 405 patients). Patients were consecutively recruited for study 1 (8 patients, 6 men, 2 women; mean age, 59 years; range, 41-74 years), and for study 2 (18 patients, 12 men, 6 women; mean age, 60 years; range, 33-76 years). The inclusion criteria were patients who had lost teeth and planned to undergo implant treatment were enrolled in the study. Radiographic examination showed vertical bone absorption, and bone augmentation was required at the site of tooth loss to perform implant treatment. The exclusion criteria were patients with diabetes, bone/joint disease or autoimmune disorder or who were taking bisphosphonates. Each patient provided written informed consent for the GBR procedure after all treatment options had been presented. The protocol of these studies was approved by the Ethics Committee of Nihon University School of Dentistry at Matsudo (EC 18-16-16-015-2).

2. Surgical procedure (study 1,2)

(1) GBR

Mineralized freeze-dried bone allograft (FDBA; LifeNet Health, Virginia Beach, USA) and autologous fibrinogen glue (AFG; made from the patient's blood) were transplanted with non-absorbable anorganic bovine bone graft material (Bio-Oss®; Geistlich Biomaterials, Wolhusen, Switzerland) into the extraction socket under local anesthesia with 36 mg of lidocaine. Non-absorbable polytetrafluoroethylene (PTFE) membrane (Cytoplast®; Osteogenics Biomedical, Lubbock, USA) was placed directly on the Bio-Oss®+FDBA+AFG (1:1:2), then an absorbable concentrated growth factor membrane 15) was extended at least 2 mm beyond the borders of the defect. Mattress and simple sutures were then placed using a suture needle with non-absorbable PTFE monofilament suture (Osteogenics Biomedical) to allow tension-free adaptation of wound margins. Minor wound dehiscence was controlled using antibiotics (flomox®; Shionogi, Osaka, Japan) and wound dressing (ConcoolF®; weltec, Osaka, Japan).

(2) Radiological interpretation of bone augmentation

Thirteen to 18 weeks after GBR, dental X-ray images were obtained under a unified standard (Max F1; Morita, Tokyo, Japan) to record bone density. To decide the time of fixture installation, the graft site on dental

films was subjectively decided by 3 dental implant specialists to estimate bone augmentation. Biopsy was performed when all 3 agreed that an implant could be placed.

(3) Biopsy and implant placement

A stainless-steel trephine burr with an external diameter of 3 mm, internal diameter of 2 mm, and length of 8-10 mm (dental trephine kit; THOMAS, Bourges, France) was used to obtain a bone core biopsy sample from the center of the GBR lesion. The excavation speed for biopsy was 300 rotations/min. Figure 1 shows images of a representative bone core sample. After removal of the bone core sample (Fig. 1a), implant osteotomy was completed, and the implant was placed according to the instructions from the implant manufacturer. Implant treatment was then completed, and stability of the implant was obtained. Clinical observation was continued after 6 months of implant placement.

(4) Preparation for analyses of bone core samples

The bone core sample (Fig. 1a) was immediately fixed in 10% neutral-buffered formalin for 7 days. In study 2, the specimen was cut along the long axis into two pieces. One piece was subjected to micro-CT and the other to histopathological examination.

3. Dental radiographic image analysis of bone augmentation (study 1)

Dental radiographic images were analyzed using ImageJ 1.51i image analysis software (NIH, Maryland, USA). Two areas of radiographic image density were measured (Fig. 2): bone augmentation area (a in Fig. 2) and existing bone just under the augmentation area (b in Fig.2). Setting of the measurement region of interest (ROI) for image analyses was decided by 2 dental radiologists to prevent inter-observer error. The relative concentration ratio of the bone augmentation area compared to the existing area (a/b) was calculated.

4. Micro-CT analysis (study 2)

Tissue samples were scanned using micro-CT (R_mCT2; Rigaku, Tokyo, Japan). Scan parameters were set to: field of view (FOV), 10 mm; tube voltage, 90 kV; and tube current, 160 μA. The image of CT was created using micro-CT equipment that generates monochromatic images with 512 × 512 pixels and a depth of 16 bits. Scanned data consisted of 512 slices. These data were exported in Digital Imaging and Communications in Medicine (DICOM) 16-bit signed format. Bone mineral density (BMD) is the amount of mineral in bone tissue. It is possible to compare, using radiological study, the amount of calcium and phosphorus deposited in the bones 16). Sample's gray value was converted to BMD by the calibration curve which was created by the gray

values of X-ray absorption from BMD phantoms (Phantoms; Ratoc System Engineering, Tokyo, Japan) comprising 200, 300, 400, 500, 600, 700, and 800 mg hydroxyapatite/cm^3.

5 Digital image analysis of bone augmentation (study 2)

Image analysis and acquisition of 3D image for bone core samples were undertaken using ImageJ. In image analysis, threshold values were set. Areas below and above the threshold values were defined in ROIs as areas of bone graft materials/new bone and soft tissue, respectively. The preliminary study was performed to set ROIs and showed a gray value ≥4,350 included all areas of the specimen other than formalin solution. Concerning bone graft materials, gray values were 6,500 for Bio-Oss® and 6,900 for FDBA. Therefore, regions of ≥6,500 were set to represent bone grafting materials and new bone tissue in the present study. BMD and tissue volume were analyzed in accordance with threshold areas. Merged 3D image for bone core biopsy was displayed with soft- and hard-tissue areas in purple and yellow, respectively.

6. Histopathological analysis (study 1,2)

The specimen was decalcified with 10% ethylenediaminetetraacetic acid for 6 days and embedded in paraffin. The paraffin-embedded block was sectioned into 7 serial sections of 4-μm thickness. The first 6 serial

sections were stained with hematoxylin and eosin (HE), and the seventh section was stained with Azan Mallory (AM).

7. Histomorphometric analysis of bone augmentation (study 1,2)

Histopathological images were captured using an optical microscope (BX51; Olympus, Tokyo, Japan) and photographic images were captured under ×40 magnification using a digital camera (DP20; Olympus). Photographic images were analyzed using ImageJ. The areas of new bone, bone graft material, and soft tissue were measured of the constant areas (718.8× 539.1 μm^2) by 2 oral pathologists. All samples were measured for six HE-stained sections (5 field of view of each to cover all the area by x10). Proportions of new bone, bone graft materials, and soft tissue 17) were calculated and expressed as percentages, and mean values, standard deviation and covariance were determined for statistical analysis.

8. Statistical analysis (study 1,2)

All statistical analyses were performed using SPSS for Windows version 20.2 J (IBM, Tokyo, Japan). The relative concentration ratio was statistically analyzed using the F test. Histomorphometric area ratios of

different tissue types within the grafted area among all cases were used for population variance analysis. In addition, the relevance of the relative concentration ratio and histomorphometric components ratio was analyzed by spearman's rank correlation coefficient. The Digital image analysis results and histomorphometric component ratios were analyzed by Pearson's correlation coefficient.

Results

1. Clinical findings (study 1,2)

The clinical information of the study subjects are shown in in Table 1 and 2. Three dental implant specialists agreed that implants could be placed at 12-20 weeks after GBR (mean, 15weeks 5 days; range, 13 weeks o day to 16 weeks 3days, study 1) and 13-19 weeks after GBR (mean, 15 weeks 4 days; range, 13 weeks 6 days to 18 weeks 1 day, study 2). In study 1 and 2, one implant was failure within 6 months after implant placement.

2. Dental radiographic image analysis of bone augmentation (study 1)

Radiographically, radiolucency of the extraction socket decreased gradually and transformed to radiopaque features corresponding to bone regeneration. The relative concentration ratios (a/b) are presented in figure 3. Sixty-seven percent of cases showed an augmentation area smaller than the existing bone area. The mean ratio was 0.92 and variance was 0.03, and no significant variability was evident among the 8 cases (p=0.48).

3. Micro-CT analysis (study 2)

Figures 4 and 5 show two representative 3D reconstructed micro-CT images of the biopsy core specimen with large (Fig. 4a, b) and medium (Fig. 5a, b) hard tissue occupancy. Soft and hard tissues showed similar

distributions to those seen from histological examination (Fig. 4c, 4d, 5c, 5d). Mean BMD was 628.11±58.00 mg/mm^3 (range, 535.50-783.10 mg/mm^3). The mean proportion of the hard tissue component on digital image was 20.09±4.91 % (range, 14.38-32.59 %).

4. Histopathological and histomorphometric findings (study 1,2)

Trabecular bone formation, osteoid continuous with the bone graft materials and mainly connective tissue were observed in the bottom, middle and upper areas, respectively (Fig. 1b). In most specimens, bone graft materials were in close contact with newly formed bone. The newly found woven bone showed a long, trabecular structure, whereas the bone graft materials were shorter and had sharper boundaries accompanied by many small lacunae, but no osteocytes. The connective tissue component was located loosely between osteoid and new woven bone and/or bone graft materials. In AM staining, new bone and osteoid stained blue, bone graft materials stained red/blue, and osteoblast/mesenchymal cells stained red (Fig. 1c).

(1) Study 1

In study 1, the histomorphometrical percentages of these components in the 8 cases are presented in Figure 6. The mean ratios of new bone, bone graft materials, osteoid and connective tissue were 15.75 ± 14.52, 21.50

± 17.31, 6.46 ± 13.36, and 56.33 ± 3.97, respectively. The average area ratio for hard tissue (i.e., new bone and bone graft materials) was 37.25 ± 11.12 %. A significant difference in percentages of these components was observed among the 8 cases according to population variance analysis (p<0.01). Histological components were also classified into three patterns of area ratio for bone graft materials in the bone core sample: large, moderate and small patterns. The large, moderate and small patterns defined as follows: the ratio for bone graft materials is over 30 %, between 3 and 29 % and less than 3 %, respectively. Typical histopathological findings for these patterns are shown in Figure 7. For all subjects, the large pattern was seen in 37.5 %, moderate in 25.0 % and small in 37.5 %.

(2) Study 2

In study 2, the percentages of these components in the 18 cases are presented in Table 3. The average proportion of the histopathological hard tissue component was 39.11 ± 9.85 % (average ± standard deviation, range 24.40-57.21 %). Mean proportions of new bone, bone graft material, osteoid and connective tissue were 15.02 ± 16.50 %, 24.09 ± 10.49 %, 5.76 ± 8.24 %, and 55.13 ± 12.68 %, respectively. A significant difference in percentages of these components was observed among the eighteen cases according to population variance

analysis (p<0.01).

(3) The relevance of the relative concentration ratio and histomorphometric components ratio (study 1)

The positive correlation with the relative concentration ratio was bone graft materials (0.595), and the negative correlation with it were observed in new bone (-0.181), osteoid (-0.548) and connective tissue (-0.252) by the spearman's rank correlation coefficient. And, correlation was indicated between the relative concentration ratio and the hard tissue area (new bone and bone graft materials) ratio (p<0.001). Conversely, an inverse correlation was indicated between the relative concentration ratio and the soft tissue area (osteoid and connective tissue) ratio (p<0.001).

(4) Relevance of digital micro-CT image and histomorphometric component ratios of bone augmentation (study 2)

A strong correlation was identified between BMD and ratios of hard tissue (new bone and bone graft material) areas on both digital micro-CT and histopathological images (correlation coefficients, 0.923 and 0.938, respectively; Fig. 8a, b, p<0.01). A positive correlation between hard tissue ratios from digital micro-CT and histopathological images (correlation coefficient, 0.875; Fig. 8c) was also confirmed (p<0.01).

Discussion

GBR has been developed for cases with insufficient bone volume, to expand the indications for dental implant treatment [1]. Sufficient radiopaque features were observed at 12-20 weeks after GBR, concordant with the description by Lee et al.[18]. Rokn et al. [2] described that one of the risk factors for implant failure was the low quality of bone, and it leads to lower treatment predictability [19]. Several kinds of techniques are available for bone density evaluation: histomorphometric analysis [2,3], Tactile sense of the surgeon [2,4], and radiological evaluation [2,5]. Radiological evaluations of bone augmentation after GBR are scarce, but measurements of new bone height have been described [7-9]. Among these previous studies, almost no objective evaluation of the subjective radiological interpretation was described. Although no statistical variability was seen among the eight cases, 67 % of all cases showed a low relative concentration ratio indicating less augmented bone than existing bone in the present study. No variation in the relative concentration ratios was considered because there was no variation in the histologic soft tissue components. Hence, bone augmentation area, where specialists clinical judged as implantation timing, was verified histopathologically. Microscopically, the mean ratios of new bone, bone graft materials, osteoid and connective tissue in study 1,2 were 15.8/15.0 %,

21.5/24.1 %, 6.5/5.8 %, and 56.3/55.1 %, respectively. Regarding the evaluation after GBR, the seven cases histomorphometrically showed proportions of new bone and residual ABB after 6 to 12 months were 39.0 % and 8 %, respectively in the sinus floor [8]. Similarly, ≥25 % [20] and 24 % to 30 % [18] of bone volume is sufficient to support implants under occlusal loads in the grafted maxillary sinus. A proportion of new bone in this result was smaller than those of previous studies [8,18,20]. On the other hand, the low rate of new bone was due to the presence of remaining nonabsorbable ABB particles [21]. Nonetheless, these bone substitutes show high rates of success with dental implants [9,22]. Anyway, it was described that a certain percentage of non-absorbable ABB remained as a component of the bone augmentation area [23]. From a histopathological perspective, bone regeneration was seen around the non-absorbable bone graft material in the 8 present cases. This finding suggested that the material acted as a nucleus of calcification and bone regeneration and was biocompatible. Besides, a strong correlation was indicated between the relative concentration ratio and the hard tissue area. A higher relative concentration ratio was not always suggestive of new bone in the present study, but bone augmentation using non-absorbable bone graft materials and new bone could be estimated from interpretation of radiological images by dentists.

Among the radiographic image techniques, micro-CT shows potential as a promising alternative to histomorphometric techniques as a method for estimating bone augmentation. BMD is used as an index for evaluating the quality of bone augmentation. A significant correlation was identified between BMD and the proportion of the hard tissue area on histopathological images in the present study. Digital image component analyses using micro-CT of areas of bone augmentation have been reported in animal models, in which the low amount of new bone could not be quantified by micro-CT [10]. Moreover, the bone regeneration effect of bone graft materials has been evaluated through micro-CT and histopathological analysis in bone defect models using dogs [11,15] and rats [12,13]. For humans, Kaigler et al. [14] reported qualitative analyses of the bone regeneration process carried out using micro-CT and histological change. The bone augmentation area has also been estimated by micro-CT, measuring some volumes within ROIs in previous studies [11-13]. However, in those studies the basis for thresholds was not clearly set [12,13] or thresholds were determined by the position in the ROI [11]. Because histological components were intermingled in bone augmentation, we assumed that the method described by Lee SH et al. [11] might be inaccurate for the present study. In the present study, the analysis target area was that area showing a gray value ≥4,350 gray value, to include all areas of the specimen other

than 10% formalin solution. Concerning bone graft materials, gray values were 6,500 for Bio-Oss® and 6,900 for FDBA in the present study. Therefore, regions of ≥6,500 were set to represent hard tissue in the present study.

Likewise, a significant correlation was seen between the hard tissue ratios from digital micro-CT and histopathological images. The mean ratio of the hard tissue component was higher for histopathological images than for digital images. Digital images seem to have a lower threshold for hard tissue in the form of new bone with little bone mineral content. These results showed the objectivity of threshold setting in the present study.

In conclusion, the present study indicated that new bone and/or reorganization with nonabsorbable ABB graft materials were observed in the bone augmentation area after GBR, and radiological interpretations by dentists were influenced by these hard tissue areas but no significant variability. Furthermore, a significant correlation was observed among histopathological analysis is of tissue components, digital analysis of tissue components and BMD. The present study showed that micro-CT can provide a good method for evaluating bone quality within a short period after bone augmentation. Studies 1 and 2 were not uniform teeth species subjects. Therefore, not be denied the limitation of this conclusion. However, correlations between the results

of component analysis from micro-CT and histomorphology have yet to be reported. The patient can understand the effect of GBR by showing 3D reorganization of bone augmentation area. Further, it may be useful for determination of implant superstructure attachment time.

References

1) Brånemark PI, Adell R, Albrektsson T, Lekholm U, Lundkvist S, et al. Osseointegrated titanium fixtures in the treatment of edentulousness. Biomaterials. 1983; 4 (1): 25-28.

2) Rokn A, Rasouli Ghahroudi AA, Daneshmonfared M, Menasheof R, Shamshiri AR. Tactile sense of the surgeon in determining bone density when placing dental implant. Implant Dent. 2014; 23 (6): 697-703.

3) Trisi P, Rao W. Bone classification: Clinicalhistomorphometric comparison. Clin Oral Implants Res. 1999; 10 (1): 1-7.

4) Herrmann I, Lekholm U, Holm S, Kultje C. Evaluation of patient and implant characteristics as potential prognostic factors for oral implant failures. Int J Oral Maxillofac Implants. 2005; 20 (2): 220-230.

5) Aranyarachkul P, Caruso J, Gantes B, Schulz E, Riggs M, et al. Bone density assessments of dental implant sites: 2. quantitative cone-beam computerized tomography. Int J Oral Maxillofac Implants. 2005; 20 (3): 416-424.

6) Katsumata A. Progress of diagnostic imaging in dentistry (in Japanese). Medical Imaging and Information Sciences. 2014; 31(4): 65-69.

7) Cricchio G, Imburgia M, Sennerby L, Lundgren S . Immediate loading of implants placed simultaneously with sinus membrane elevation in the posterior atrophic maxilla: A two-year follow-up study on 10 patients. Clin Implant Dent Relat Res. 2014; 16 (4): 609-917.

8) Ferreira CE , Novaes A B, Haraszthy VI, Bittencourt M, Martinelli CB, et al. A clinical study of 406 sinus augmentations with 100% anorganic bovine bone. J Periodontol. 2009; 80 (12): 1920-1927.

9) Dinato TR, Grossi ML, Teixeira ER, Dinato JC, Sczepanik FS, et al. Marginal bone loss in implants placed in the maxillary sinus grafted with anorganic bovine bone: A prospective clinical and radiographic study. J Periodontol. 2016; 87(8): 880-887.

10) Fuegl Al, Tangl S, Keibl C, Watzek G, Redl H, et al. The impact of ovariectomy and hyperglycemia on graft consolidation in rat calvaria. Clin Oral Implants Res. 2011; 22 (5): 524-529.

11) Lee SH, An SJ, Lim YM, Huh JB. The efficacy of electron beam irradiated bacterial cellulose membranes as compared with collagen membranes on guided bone regeneration in periimplant bone defects. Materials (Basel). 2017; 10 (9): pii:E1018.doi: 10.3390/ma10091018.

12) Kaigler D, Krebsbach PH, Wang Z, West ER, Horger K, et al. Transplanted endothelial cells enhance

orthotopic bone regeneration. J Dent Res. 2006; 85 (7): 633-637.

13) Park CH, Abramson ZR, Taba M Jr, Jin Q, Chang J, et al. Three-dimensional micro-computed tomographic imaging of alveolar bone in experimental bone loss or repair. J Periodontol. 2007; 78 (2): 273-281.

14) Kaigler D, Pagni G, Park CH, Braun TM, Holman LA, et al. Stem cell therapy for craniofacial bone regeneration: a randomized, controlled feasibility trial. Cell Transplant. 2013; 22 (5): 767-777.

15) Hu H, Pu Y, Lu S, Zhang K, Guo Y, et al. The osteogenesis effect and underlying mechanisms of local delivery of gAPN in extraction sockets of beagle dogs. Int J Mol Sci. 2015; 16 (19): 24946-24964.

16) Almeida Paz ICL, Bruno LDG. Bone mineral density: review. Braz J Poultry Sci. 2006; 8 (2): 69-73.

17) Choi SY, Jang YJ, Choi JY, Jeong JH, Kwon TG. Histomorphometric analysis of sinus augmentation using bovine bone mineral with two different resorbable membranes. Clin Oral Implants Res. 2013; 24 (Suppl A100): 68-74.

18) Lee CY, Prasad HS, Suzuki JB, Stover JD, Rohrer MD. The correlation of bone mineral density and histologic data in the early grafted maxillary sinus: a preliminary report. Implant Dent. 2011; 20 (3): 202-214.

19) Alsaadi G, Quirynen M, Michiels K, Jacobs R, van Steenberghe D. A biomechanical assessment of the relation between the oral implant stability at insertion and subjective bone quality assessment. J Clin Periodontol. 2007; 34 (4): 359-366.

20) Froum SJ, Tarnow DP, Wallace SS, Jalbout Z, Cho SC, et al. The use of a mineralized allograft for sinus augmentation: an interim histological case report from a prospective clinical study. Compend Contin Educ Dent. 2005; 26 (4): 259-260.

21) Bonardi JP, Pereira RDS, Boos Lima FBDJ, Faverani LP, Griza GL, et al. Prospective and randomized evaluation of ChronOS and Bio-Oss® in human maxillary sinuses: histomorphometric and immunohistochemical assignment for Runx 2, vascular endothelial growth factor, and osteocalcin. J Oral Maxillofac Surg. 2018; 76 (2): 325-335.

22) Galindo-Moreno P, Padial-Molina M, Fernández-Barbero JE, Mesa F, Rodríguez-Martínez D, et al. Optimal microvessel density from composite graft of autogenous maxillary cortical bone and anorganic bovine bone in sinus augmentation: influence of clinical variables. Clin Oral Implants Res. 2010; 21 (2): 221-227.

23) Utsunomiya T, Hayashi M, Murakami H, Nakamoto D, Fukushima T, et al. Histopathological evaluation

of growth factor-rich fibrin combined with anorganic bone graft materials and atelocollagen in a human extraction socket: a case report. Int J Oral-Med Sci. 2016; 15 (1): 22-27.

Figure legend

Figure 1　Macroscopic（a）and loupe images of the biopsy specimen（b：hematoxyline and eosin staining (HE)；c：Azan Mallory stain(AM)).

Red zone indicates mucosal surface（a）

Figure 2　Setting of measurement ROI for dental radiographic image analysis of the bone augmentation area（a：broken line square, bone augmentation area ; b：dotted line square, existing bone just under the augmentation area).

Figure 3　Relative concentration ratios in all cases. Average ratio was 0.92, and 67% of cases showed a relative concentration ratio below 1, indicating a bone augmentation area smaller than the existing bone area.

Figure 4　Representative images of biopsy core sample with a large proportion of hard tissue a,b) 3D reconstructed micro-CT images (c: hard tissue in yellow; d: merged image with soft tissue in purple and hard tissue in yellow) ; and c,d) histological findings of bottom area (×10; c: HE; d: AM, scale bur: 100um). Bottom and upper sides of figures (a,b) presents existing bone and mucosal direction, respectively.

Figure 5　Representative images of biopsy core sample with a medium proportion of hard tissue

a,b) 3D reconstructed micro-CT images (c: hard tissue in yellow; d: merged image with soft tissue in purple and hard tissue in yellow); and c,d) histological findings of bottom area (×10；e： HE, f: AM, scale bur: 100um). Bottom and upper sides of figures (a, b) presents existing bone and mucosal direction, respectively.

Figure 6　Percentages of tissue components in all cases of experiment 1.

Figure 7　Typical findings for three patterns of area ratio for bone graft materials in the biopsy specimen: large (A), moderate (B) and small patterns (C).

A1-C1：Histopathological pictures（HE, x20）

A2-C2：Histopathological pictures（AM, x20）

A3-C3：Proportion of bone graft materials in bone augmentation area

Figure 8

a）Correlation between bone mineral density（BMD） and hard tissue（new bone and bone graft material）component ratio from digital micro-CT images.

b）Correlation between BMD and hard tissue（new bone and bone graft material）component ratio from histopathological images.

c）Correlation between hard tissue（new bone and bone graft material）component ratios from digital micro-CT and histopathological images

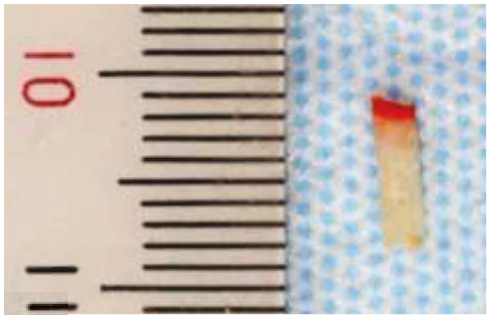

a

Fig.1

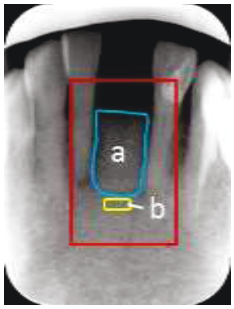

Fig.2

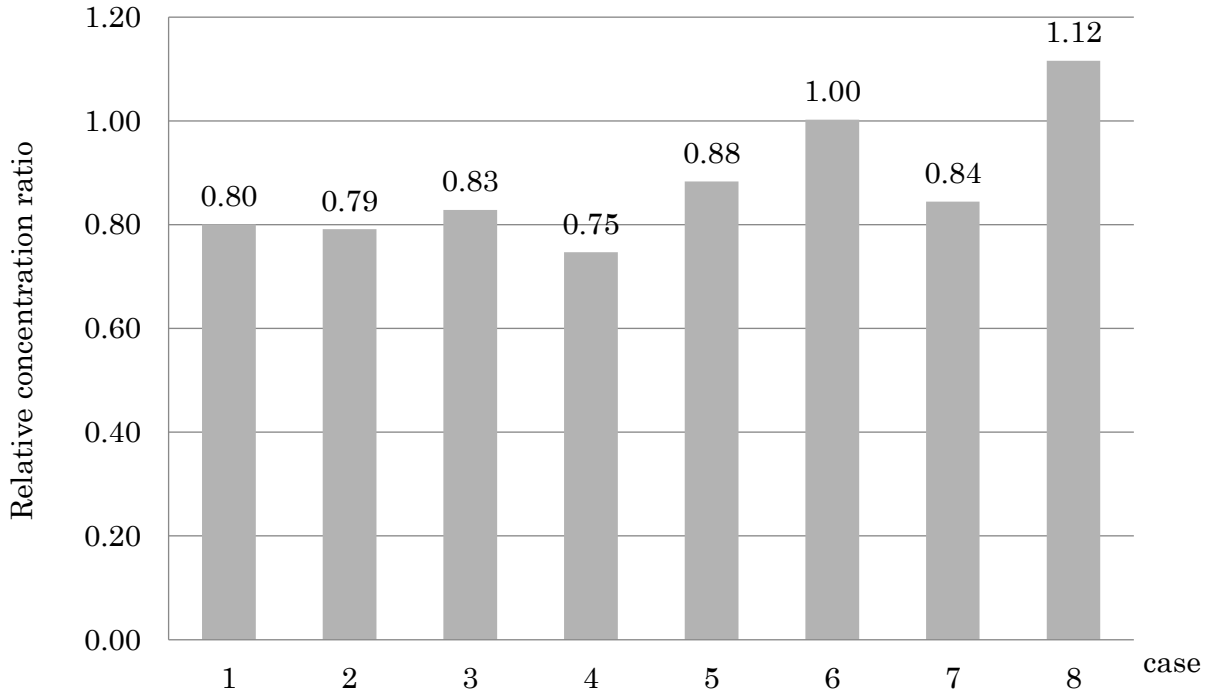
Relative concentration ratio
1.20
1.00
0.80
0.60
0.40
0.20
0.00
0.80
0.79
0.83
0.75
0.88
1.00
0.84
1.12
1
2
3
4
5
6
7
8
case

Fig.3

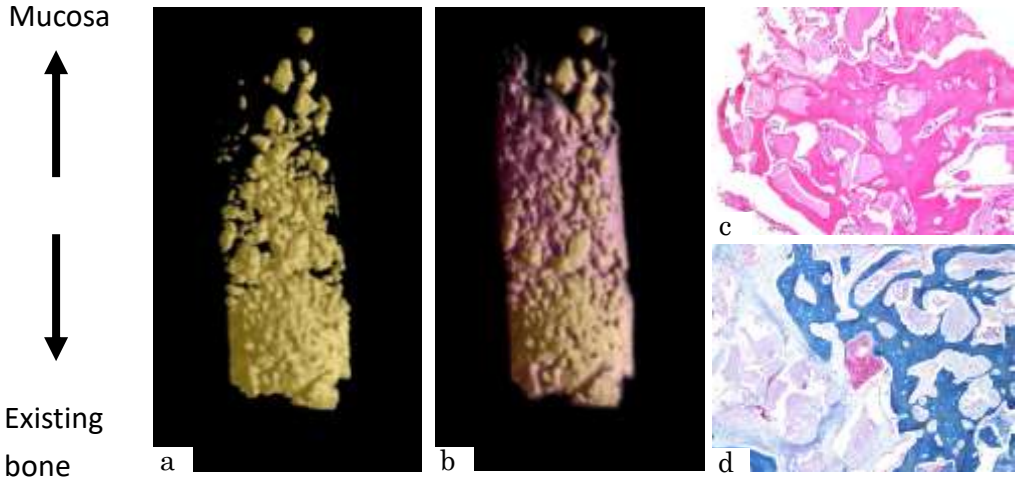

Fig.4

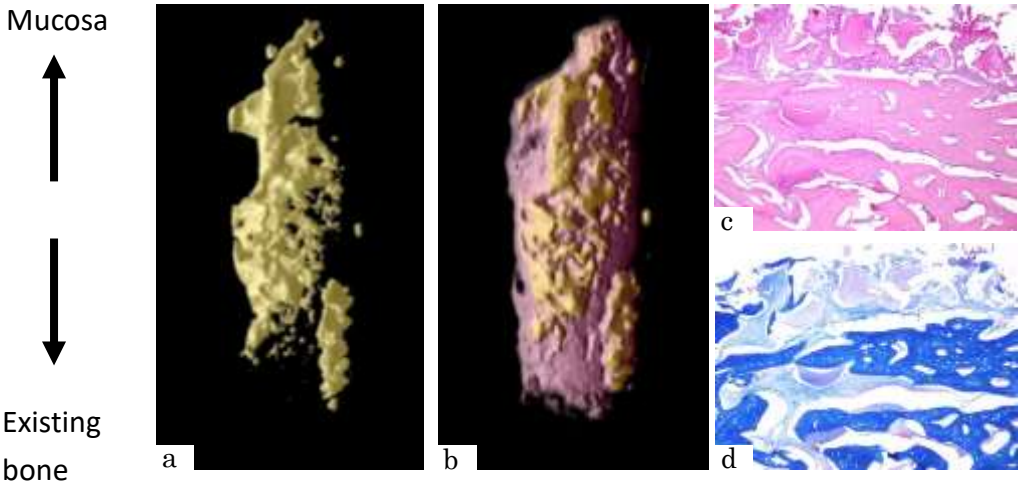

Fig.5

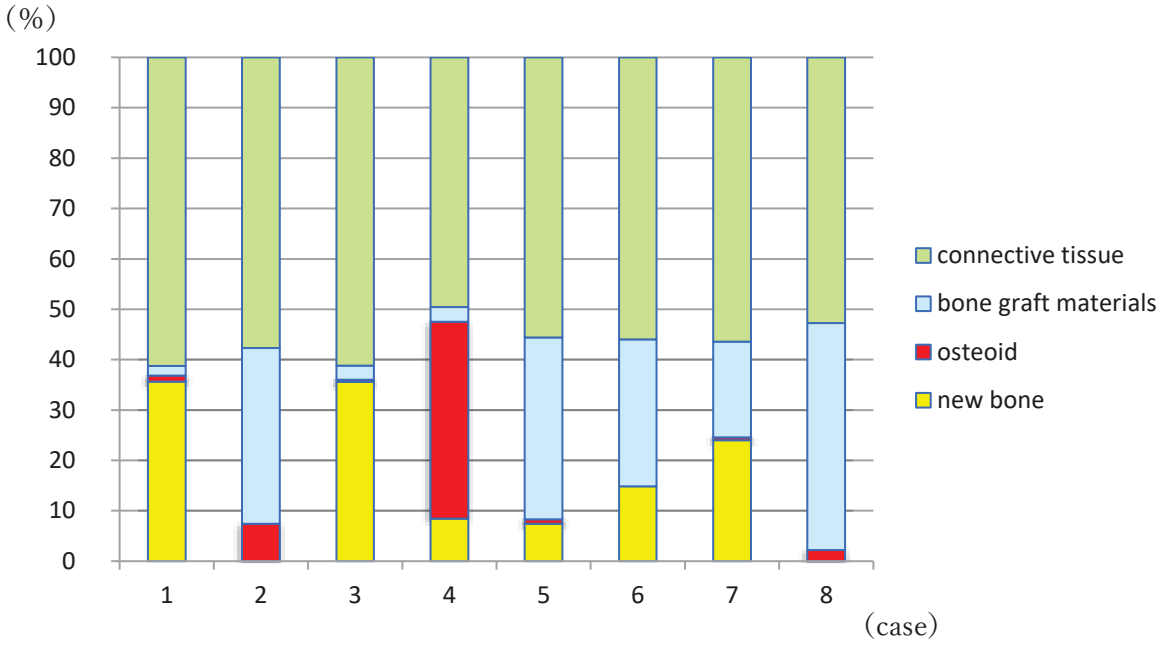
(%)
100
90
80
70
60
50
40
30
20
10
0
1
2
3
4
5
6
7
8
(case)
connective tissue
bone graft materials
osteoid
new bone

Fig.6

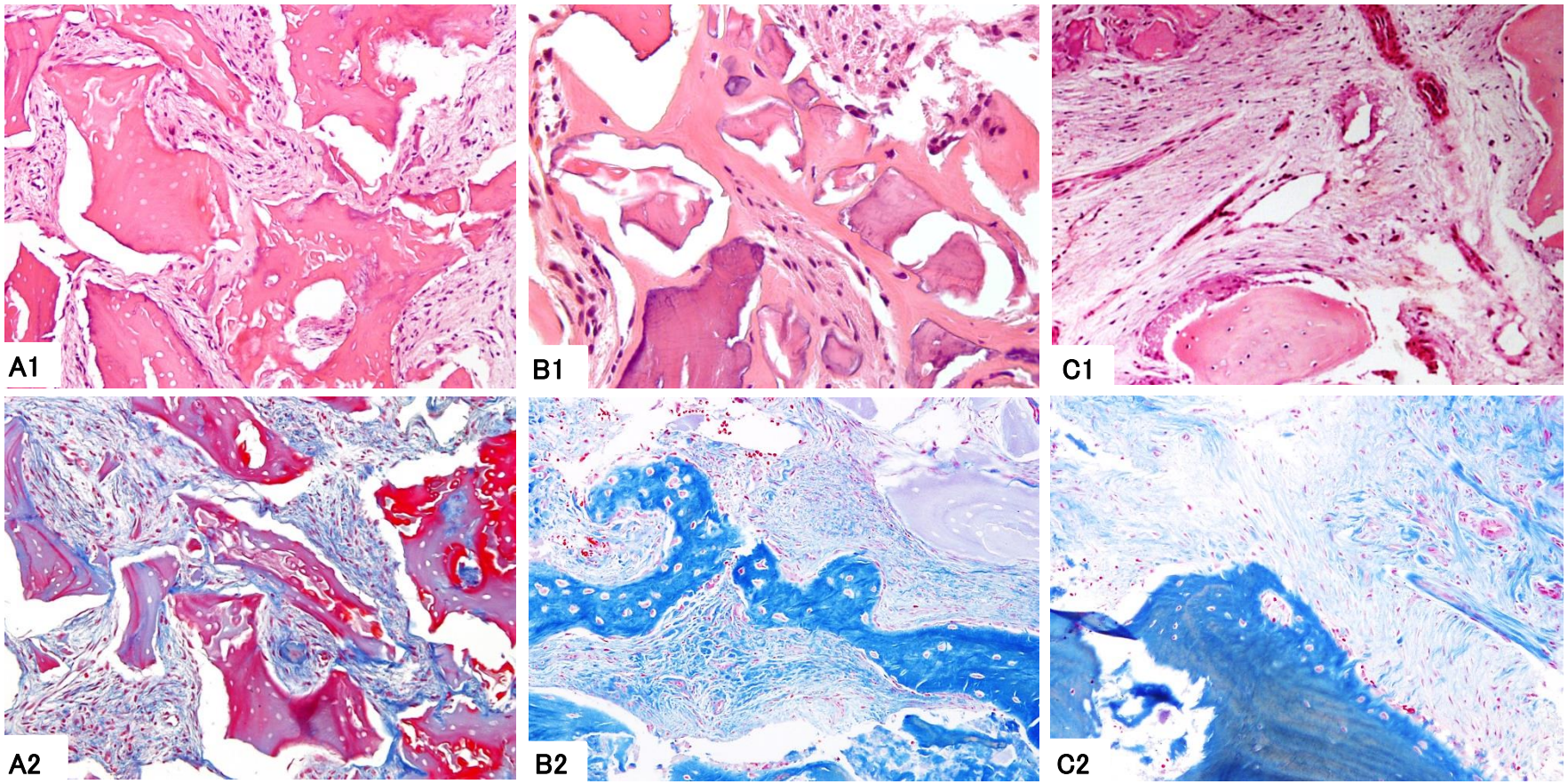
A1
B1
C1
A2
B2
C2
2.50
3.50
38.73
55.47
A3
19.45
0.30
24.10
56.20
B3
26.53
13.53
57.27
2.53
C3
connective tissue
bone graft materials
osteoid
new bone

Fig.7

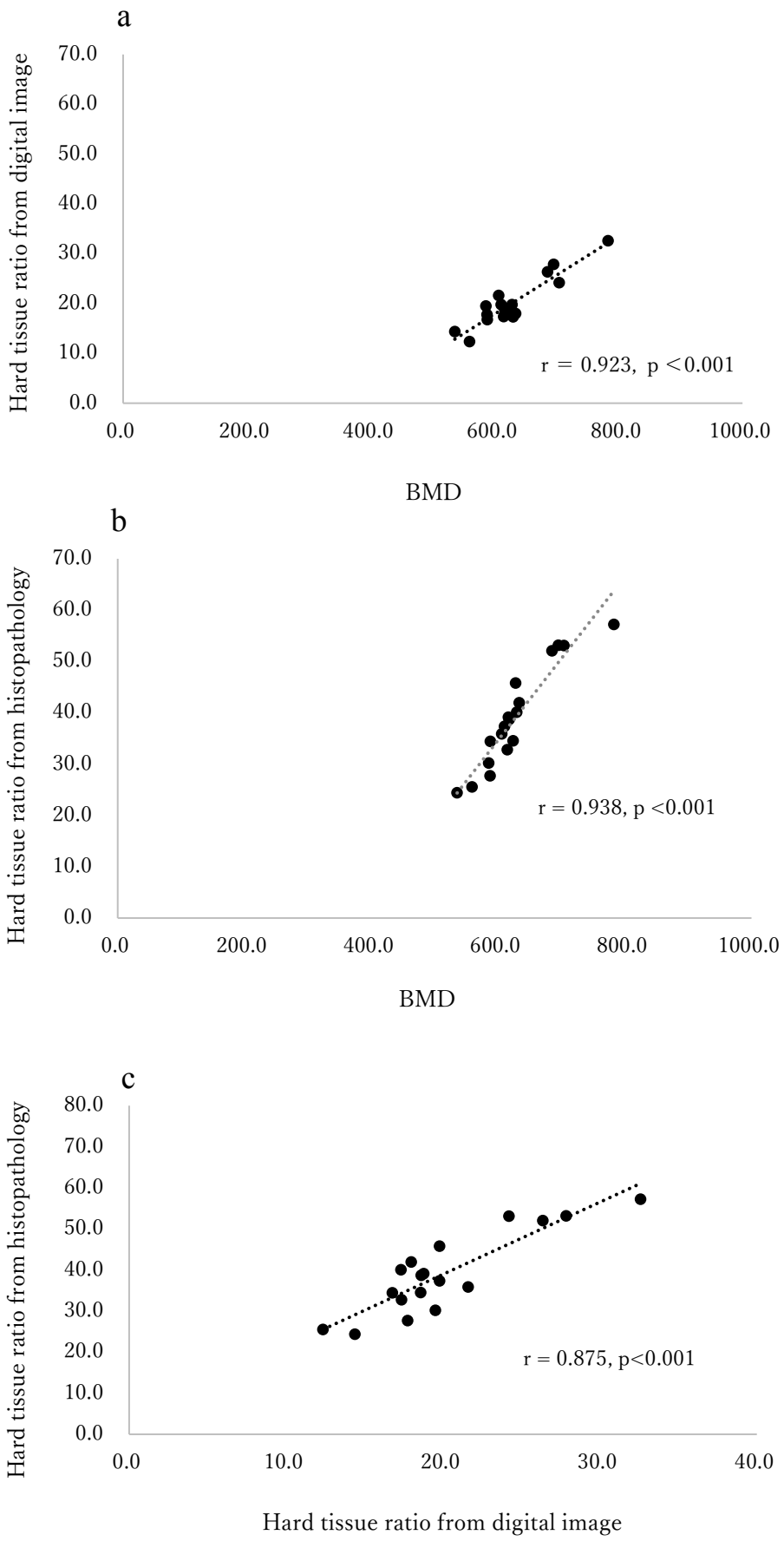
a
Hard tissue ratio from digital image
70.0
60.0
50.0
40.0
30.0
20.0
10.0
0.0
0.0
200.0
400.0
600.0
800.0
1000.0
BMD
r = 0.923, p <0.001
b
Hard tissue ratio from histopathology
70.0
60.0
50.0
40.0
30.0
20.0
10.0
0.0
0.0
200.0
400.0
600.0
800.0
1000.0
BMD
r = 0.938, p <0.001
c
Hard tissue ratio from histopathology
80.0
70.0
60.0
50.0
40.0
30.0
20.0
10.0
0.0
0.0
10.0
20.0
30.0
40.0
Hard tissue ratio from digital image
r = 0.875, p<0.001

Fig. 8

Table 1　List of cases

Case	Sex	Age(years)	Missing teeth[1]	Period[2]
1	M	43	11	3m3w
2	F	68	21	3m2w
3	F	55	27	5m0w
4	M	65	35	3m0w
5	M	74	11	3m2w
6	M	56	27	5m0w
7	M	70	41	3m2w
8	M	41	15	3m3w

1: FDI two-digit system tooth number

2: Period after guided bone regeneration

Table 2　List of cases

Case	Sex	Age (years)	Missing teeth[1]	Period[2]
1	M	44	24	3m1w
2	M	55	45,45	3m3w
3	M	62	11,12	3m3w
4*	M	42	15	4m0w
5	M	76	11	3m2w
6	M	68	15	3m3w
7	M	68	26	3m2w
8	M	73	46	3m1w
9	M	75	13	3m3w
10	F	33	16	4m0w
11	F	61	36	4m0w
12	F	61	44	4m0w
13	M	60	46	4m1w
14	F	68	46	4m2w
15	F	61	22	3m2w
16	F	67	36	3m2w
17	M	52	21	4m2w
18	M	56	36	4m1w

1: FDI two-digit system tooth number

2: Period after guided bone regeneration

*: Case 4 showed implant treatment failure within 6 months after implant placement.

Table 3 Histopathological components in all cases (%)

Case	**Hard tissue***	New bone	Bone graft materials	**Soft tissue****	Osteoid	Connective tissue
1	**57.21**	50.00	7.21	**42.79**	3.18	39.61
2	**34.45**	0.00	34.45	**65.55**	6.18	59.37
3	**30.18**	0.17	30.01	**69.82**	4.77	65.05
4	**35.89**	3.50	32.39	**64.11**	1.11	63.00
5	**25.53**	0.00	25.53	**74.47**	0.61	73.86
6	**32.77**	3.10	29.67	**67.23**	5.75	61.48
7	**27.69**	16.66	11.03	**72.31**	8.09	64.22
8	**37.34**	12.73	24.61	**62.66**	7.01	55.65
9	**41.95**	9.55	32.40	**58.05**	1.67	56.38
10	**45.80**	9.46	36.34	**54.20**	1.76	52.44
11	**24.40**	0.00	24.40	**75.60**	3.44	72.16
12	**34.54**	0.00	34.54	**65.46**	1.92	63.54
13	**39.11**	31.61	7.50	**60.89**	37.59	23.30
14	**53.09**	48.29	4.80	**46.91**	3.69	43.22
15	**40.08**	4.78	35.30	**59.92**	1.67	58.25
16	**53.17**	30.82	22.35	**46.83**	4.59	42.24
17	**52.04**	27.05	24.99	**47.96**	4.59	43.37
18	**38.69**	22.70	15.99	**61.31**	6.15	55.16

* Hard tissue represents areas of new bone and bone graft materials

** Soft tissue represents areas of osteoid and connective tissue